Scientific Research Publishing

International Journal of Astronomy and Astrophysics, 2026, 16(1), 11-24
https://www.scirp.org/journal/ijaa
ISSN Online: 2161-4725
ISSN Print: 2161-4717

Estimate of the Warm Dark Matter Free-Streaming Cut-Off with Isolated Dwarf Galaxies in the Local Field

Bruce Hoeneisen

Universidad San Francisco de Quito, Quito, Ecuador
Email: bhoeneisen@usfq.edu.ec

How to cite this paper: Hoeneisen, B. (2026) Estimate of the Warm Dark Matter Free-Streaming Cut-Off with Isolated Dwarf Galaxies in the Local Field. *International Journal of Astronomy and Astrophysics*, **16**, 11-24.
https://doi.org/10.4236/ijaa.2026.161002

Received: November 11, 2025
Accepted: January 24, 2026
Published: January 27, 2026

Abstract

The standard cold dark matter ΛCDM cosmology model is a triumph of modern physics. However, it predicts an excess of isolated dwarf galaxies in the field. Warm dark matter is an alternative that reduces the predicted number density of dwarf galaxies. We obtain the warm dark matter free-streaming cut-off wavevector k_{fs} from the number density of isolated dwarf galaxies in the Local Field with data of the *Local Volume Database* (LVDB) catalog. k_{fs} is defined as follows: $P_{\Lambda\text{CDM}}(k)\exp\left(-k^2/k_{\text{fs}}^2\right)$ is the linear density power spectrum, before first galaxies, *i.e.*, before re-generation of small-scale perturbations, referred to the present time. We obtain $k_{\text{fs}} = 2.5^{+1.8}_{-1.9}\ \text{Mpc}^{-1}$, with 68% confidence. This result is in agreement with previous measurements, but in disagreement with published limits.

Keywords

Warm Dark Matter, Dwarf Galaxies, Free Streaming

1. Introduction

We focus our attention on the number density of isolated dwarf galaxies in the Local Field because it might tell us something about the nature of dark matter. Most matter in the universe is in a "dark matter" form that has only been "observed" through its gravitational interaction [1]. In the current ΛCDM cosmology model, dark matter is a gas so cold that the dispersion velocity of the dark matter particles has a negligible effect on cosmological observations [1]. Nevertheless, we would like to know just how warm dark matter is to be able to make sensible extrapolations to the past, and also to perhaps understand several tensions of the ΛCDM cosmology

on small scales [1], such as the large excess of predicted dwarf galaxies in the Local Field (see Section 5 below). We assume that dark matter is a gas of particles of mass m_h. The "warmness" of dark matter can be specified by several related parameters, e.g., the comoving root-mean-square velocity $v_{h\mathrm{rms}}(1)$, the comoving linear density power spectrum cut-off wavevector k_{fs} due to free-streaming, or the "standard thermal relic mass" m_{th}. $v_{h\mathrm{rms}}(1)$ is defined as

$$v_{h\mathrm{rms}}(1) \equiv v_{h\mathrm{rms}}(a)\,a = v_{h\mathrm{rms}}(a)\left(\frac{\Omega_c \rho_{\mathrm{crit}}}{\rho_h(a)}\right)^{1/3}. \tag{1}$$

$v_{h\mathrm{rms}}(a)$ is the root-mean-square non-relativistic thermal velocity of dark matter particles in the early, nearly homogeneous universe at expansion parameter $a(t)$. The corresponding dark matter density is $\rho_h(a)$. The expansion parameter is normalized to $a(t_0)=1$ at the present time t_0. At the present time, the dark matter density is $\rho_h(1)=\Omega_c\rho_{\mathrm{crit}}$. Since $v_{h\mathrm{rms}}(a)$ is proportional to a^{-1} and $\rho_h(a)\propto a^{-3}$, $v_{h\mathrm{rms}}(1)$ is an adiabatic invariant.

Warm dark matter particles free-stream in and out of density minimums and maximums, thereby erasing small-scale density fluctuations. Let $P_{\Lambda\mathrm{CDM}}(k)$ be the well-known comoving linear density power spectrum of ΛCDM cosmology, before the first galaxies, *i.e.*, before non-linear re-generation of small-scale structure. k is the present time wavevector. Then, the comoving linear power spectrum in the warm dark matter model is $P_{\Lambda\mathrm{WDM}}(k)=P_{\Lambda\mathrm{CDM}}(k)\tau^2(k)$, where $\tau^2(k)$ is a cut-off factor of the form $\tau^2(k)=\exp\left(-k^2/k_{\mathrm{fs}}^2\right)$ if dark matter has the Maxwell distribution of velocities [2]. This is our definition of k_{fs} (alternative definitions in the literature are $\tau^2(k_{\mathrm{fs}})=1/2$ or 1/4). The relation between $v_{h\mathrm{rms}}(1)$ and k_{fs} (at a time t_{gal} before the first galaxies and the corresponding non-linear re-generation of density fluctuations) is [2] [3]

$$k_{\mathrm{fs}}(t_{\mathrm{gal}}) = 0.88\sqrt{\frac{4\pi G\Omega_m \rho_{\mathrm{crit}} a_{\mathrm{eq}}}{v_{h\mathrm{rms}}^2(1)}} = 1.41\ \mathrm{Mpc}^{-1}\,\frac{493\ \mathrm{m/s}}{v_{h\mathrm{rms}}(1)} \tag{2}$$

if dark matter particles have the Maxwell velocity distribution. The relation between the "standard thermal relic mass" m_{th} and k_{fs} is often defined by Equation (6) and Equation (7) of [4]. Note that the actual mass m_h is model-dependent [5].

A summary of *measurements* of $v_{h\mathrm{rms}}(1)$ can be found in [5]. A summary of *limits* on m_{th} is presented in Figure 3 of [6], see references therein. These limits on m_{th} place corresponding limits on k_{fs} and $v_{h\mathrm{rms}}(1)$ summarized in Table 2 of [7]. It turns out that there is a discrepancy between these measurements and limits that is not currently understood. The tightest limit on k_{fs} is obtained from the number counts of satellites of the Milky Way. Here, we attempt to estimate k_{fs} in the arguably simplest setting: we compare predictions with the observed number of isolated dwarf galaxies in the Local Field. Most of these dwarf galaxies are "red and dead", *i.e.*, old, and some are young and blue with stars in the main sequence, so their age has a wide distribution [8]. The isolated dwarf galaxies have

generally not experienced mergers or accretions, and are not "stripped down" galaxies that have lost matter to neighboring hosts during their formation and hierarchical evolution. Counting isolated dwarf galaxies in the Local Field avoids the need to understand the formation and evolution of the Milky Way with its satellites in the warm dark matter scenario. Our main interest is to understand the discrepancy mentioned above. Therefore, we present this analysis in full detail, so the reader can check each step of the way (that is often not possible with the published limits). Isolated dwarf galaxies in the Local Field may be first-generation galaxies, a concept valid if dark matter is warm, and will surely teach us something.

2. The Data

We study the "Local Field" dwarf galaxies in the *Local Volume Database* (LVDB) catalog [9] (in file *read_comb_all.csv* of October 11, 2025). A handy application (https://lvd-interactive.streamlit.app/) is available to visualize the distributions of the dwarf galaxies classified as Milky Way Dwarfs, M31 Dwarfs, Local Field Dwarfs, Distant Local Field Dwarfs, Globular Clusters, etc. The Local Field Dwarfs are defined to be at a distance less than 3 Mpc from the Sun, and are unassociated with the Milky Way or with M31. The catalog is complete for all *known* dwarf galaxies in the Local Field. Beyond the Local Field, the catalog is not complete. The multiple (and sometimes ambiguous) criteria to define a star cluster as a dwarf galaxy are listed in the catalog. The Local Field has 64 dwarf candidates, of which 55 are confirmed-real and confirmed-dwarf. We do not consider 11 of these dwarf galaxies because they are satellites of a host galaxy. Of the remaining 44 isolated dwarf galaxies, 42 are contained in the volume 6 Mpc × 6 Mpc × 2 Mpc defined in **Figure 1**, and within 3 Mpc of the Sun, and excluding the volumes assigned to the Milky Way and M31, leaving 56.5 Mpc^3. The corresponding number density is 0.743 $(1 \pm 42^{-1/2})$ isolated dwarf galaxies per Mpc^3. The Milky Way lies at the center of **Figure 1**, but is not shown. The stellar mass distribution is presented in **Figure 2**. The stellar mass is obtained from the absolute magnitude M_V in the V-band, assuming a mass-to-light ratio twice the solar ratio. We will assume that the distribution of stellar masses presented in **Figure 2** is cut-off at the lower end, so the number density of dwarf galaxies in the Local Field is well defined (this assumption needs to be re-evaluated in the end). The volume of **Figure 1** contains larger galaxies, notably the Milky Way and M31 with their satellites, as well as 11 smaller hosts, which are not shown nor counted.

A few of the dwarf galaxies in the Local Field have a measured line-of-sight velocity dispersion measurement. However, we do not use this information in the present analysis, we use only the number density in order to obtain an estimate of k_{fs} that is independent of measurements based on rotation curves, line-of-sight velocity dispersions or stellar dynamics.

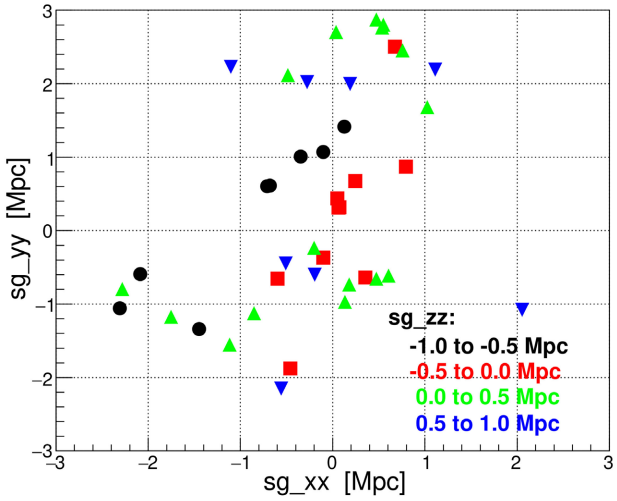

Figure 1. Supergalactic coordinates of 42 confirmed-real and confirmed-dwarf isolated galaxies in the Local Field, from the LVDB catalog [9]. The Milky Way (not shown) is at the center.

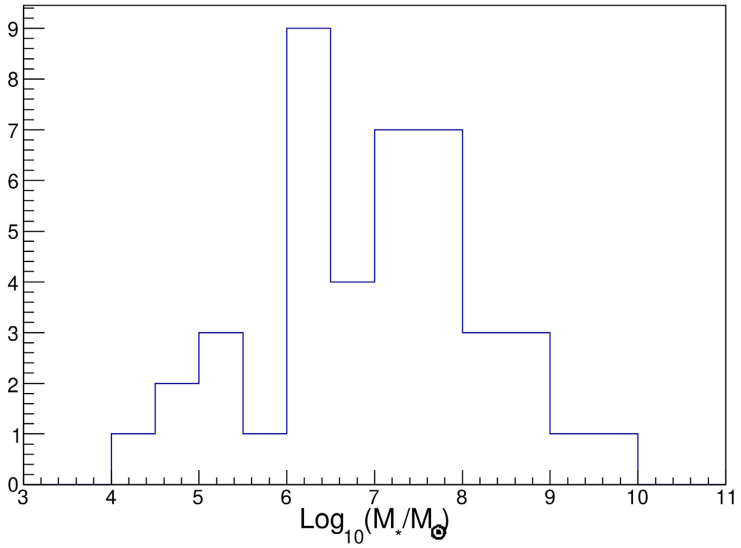

Figure 2. Stellar mass distribution of 42 isolated Local Field dwarf galaxies from the LVDB catalog [9] (that are confirmed-real and confirmed-dwarf).

3. Estimate

What can we learn from **Figure 1**? The number density of isolated dwarf galaxies in the Local Field is $1/(1.1\ \text{Mpc})^3$. So a typical nearest neighbor distance is 1.1 Mpc. This means that the warm dark matter power spectrum $P_{\Lambda\text{CDM}}(k)\exp\left(-k^2/k_{\text{fs}}^2\right)$ is non-negligible at $k = 2\pi/(1.1\ \text{Mpc}) = 5.7\ \ \text{Mpc}^{-1}$, so k_{fs} can not be very much smaller than 5.7 Mpc^{-1}.

Cold dark matter predicts a number density of dwarf galaxies much greater than observed (see Section 5). This is one of the reasons to consider warm dark matter. To reduce the number density of dwarf galaxies significantly, k_{fs} can not be very much greater than 5.7 Mpc^{-1}.

Therefore, we make the following order-of-magnitude estimate:

$$k_{\text{fs}} \approx 5.7 \text{ Mpc}^{-1}. \tag{3}$$

4. Analysis

Let us establish the notation [1]. The relative over-density at the present time is $\delta(\boldsymbol{x}) \equiv \big(\rho(\boldsymbol{x}) - \langle\rho\rangle\big)/\langle\rho\rangle$. We apply periodic boundary conditions to a large cube of volume L^3. Then, the wavevector has discrete values $\boldsymbol{k} = (2\pi/L)\big(n\boldsymbol{e}_x + m\boldsymbol{e}_y + l\boldsymbol{e}_z\big)$, so $k \equiv |\boldsymbol{k}| = (2\pi/L)\sqrt{n^2+m^2+l^2}$. The relative over-density may be written as

$$\delta(\boldsymbol{x}) = \sum_{8o.} \delta_{\boldsymbol{k}} \mathrm{e}^{-i\boldsymbol{k}\cdot\boldsymbol{x}} = \sum_{8o.} \delta^*_{\boldsymbol{k}} \mathrm{e}^{i\boldsymbol{k}\cdot\boldsymbol{x}}, \tag{4}$$

where the sums are over 8 octants of $\boldsymbol{k}$. Taking $\delta_{\boldsymbol{k}} = \delta^*_{-\boldsymbol{k}} \equiv |\delta_{\boldsymbol{k}}| \mathrm{e}^{-i\phi}$ obtains

$$\delta(\boldsymbol{x}) = \sum_{4o.} 2|\delta_{\boldsymbol{k}}| \cos(\boldsymbol{k}\cdot\boldsymbol{x} + \phi). \tag{5}$$

The variance of the density defines the power spectrum $P(k)$:

$$\big\langle \delta(\boldsymbol{x})^2 \big\rangle = \sum_{8o.} |\delta_{\boldsymbol{k}}|^2 \equiv \frac{1}{(2\pi)^3} \int P(k)\, \mathrm{d}^3\boldsymbol{k} = \frac{1}{2\pi^2} \int_0^\infty P(k) k^2 \mathrm{d}k, \tag{6}$$

so

$$|\delta_{\boldsymbol{k}}|^2 = P(k)/L^3, \tag{7}$$

with $P(k)$ in units Mpc^3. Brackets denote volume averages. In detail, at the present time, and in the linear approximation (that has already broken down), we take

$$\begin{aligned} \delta(x,y,z) = \delta_{\text{B}} + \sum_{n,m,l=2}^{49} 2|\delta_{\boldsymbol{k}}| \Big\{ & \cos\big[(2\pi/L)(nx+my+lz) + \phi_1(n,m,l)\big] \\ & + \cos\big[(2\pi/L)(-nx+my+lz) + \phi_2(n,m,l)\big] \\ & + \cos\big[(2\pi/L)(nx-my+lz) + \phi_3(n,m,l)\big] \\ & + \cos\big[(2\pi/L)(nx+my-lz) + \phi_4(n,m,l)\big] \Big\} \end{aligned} \tag{8}$$

where

$$|\delta_{\boldsymbol{k}}| = \sqrt{\frac{P_{\Lambda\text{CDM}}(k)\tau^2(k)}{L^3}}. \tag{9}$$

For our simulations, we take $L = 10$ Mpc. δ_{B} is the relative over-density of the Local Volume, and fills in for wavevectors less than $\sqrt{3}\cdot 4\pi/L$. We take $\delta_{\text{B}} = 0$, and in the end, add a systematic uncertainty on k_{fs} to include the uncertainty of δ_{B}. The $\phi_i(n,m,l)$ with $i = 1,2,3,4$ are random phases between 0 and 2π. These phases are generated with a common seed, so that runs with different coordinate sg_zz can be compared. The linear power spectrum $P_{\Lambda\text{CDM}}(k)$ extrapolated to the present time is taken from the analytical expression (Equation (8.1.42) of [10]) with a spectral index slope $n_s = 0.965$ and an amplitude normalized to $\sigma_8 = 0.811$ [1]. As a cross-check, we present this power spectrum in **Figure 3**.

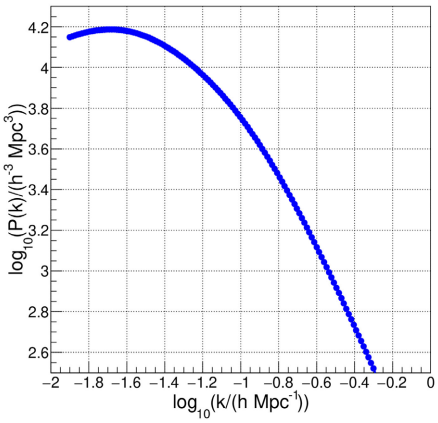

Figure 3. Present-day linear power spectrum of ΛCDM cosmology (from Equation (8.1.42) of [10] with $n_s = 0.965$ and normalized to $\sigma_8 = 0.811$) [1].

5. Upper Bound

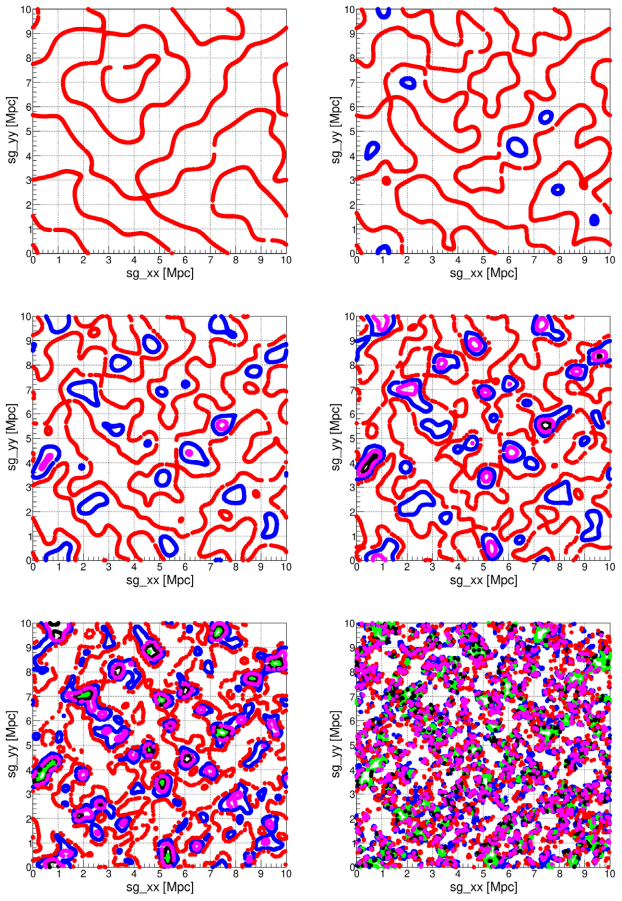

Figure 4. Simulations at redshift $z = 0$ with $k_{fs} = 2,3,4,5,7$ and 20 Mpc^{-1}. Shown are contours of constant relative overdensity: $\delta(\boldsymbol{x}) = 0$ red, 1.69 blue, 3 redish, 4 black, and 5 green, in the linear approximation (that has already broken down). Some of these contours may be omitted for clarity. The coordinates are supergalactic. sg_zz = 2.5 Mpc.

Here, we neglect non-linear re-generation of small-scale structure after the formation

of the first galaxies. Therefore, the measurement in this section obtains an upper bound to k_{fs}. Here, we also neglect a possible Local Volume over-density or under-density, *i.e.*, we set $\delta_{\mathrm{B}} = 0$. To illustrate the sensitivity of the measurement of k_{fs}, we present simulations with several k_{fs} at redshift $z = 0$ in **Figure 4**, and at redshift $z = 4$ in **Figure 5**. Let us recall that a spherically symmetric perturbation that reaches a relative over-density $\delta = 1.686$ in the linear approximation (that has already broken down) has an exact solution that diverges. Comparing the simulations in **Figure 4** with **Figure 1**, we conclude that $4 \lesssim k_{\mathrm{fs}} \lesssim 7$ Mpc^{-1}. Since more than half of the dwarf galaxies are "red and dead" [8], *i.e.*, old, we estimate $4 \lesssim k_{\mathrm{fs}} \lesssim 10$ Mpc^{-1} from **Figure 5** corresponding to $z = 4$. From **Figure 4** and **Figure 5**, we also confirm that the ΛCDM scenario, with $k_{\mathrm{fs}} > 20$ Mpc^{-1}, obtains too many dwarf galaxies in the Local Field, and therefore consider warm dark matter as a possible solution to this problem.

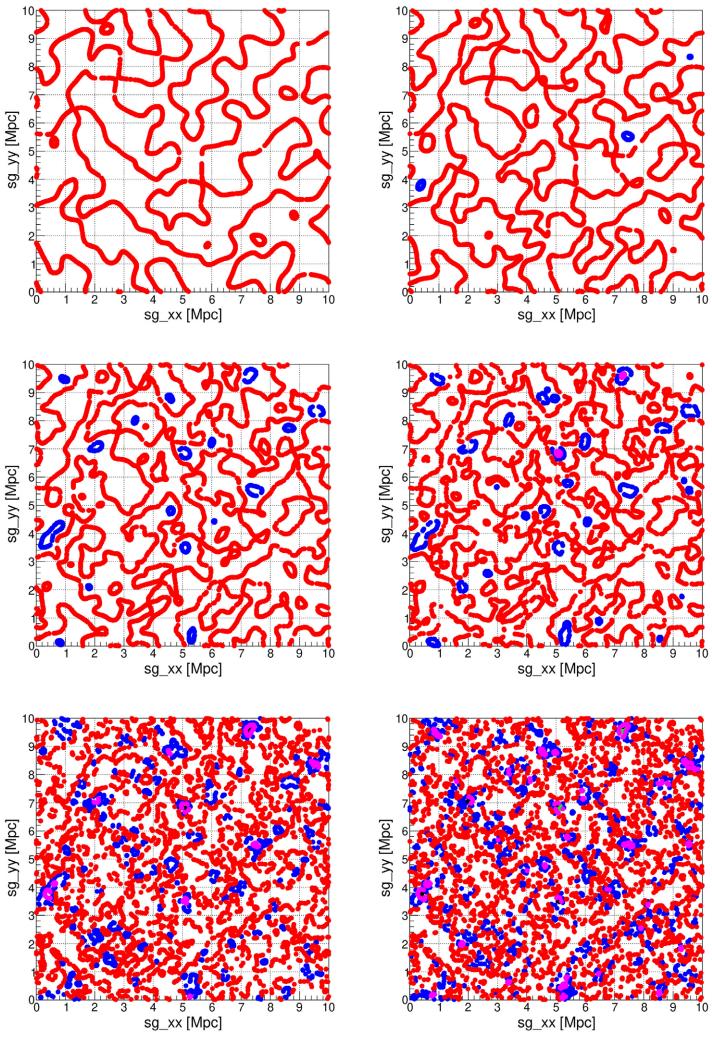

Figure 5. Simulations at redshift $z = 4$ with $k_{\mathrm{fs}} = 4, 6, 8, 10, 15$ and 20 Mpc^{-1}. Shown are contours of constant relative over-density: $\delta(\boldsymbol{x}) = 0$ red, 1.69 blue, and 3 redish, in the linear approximation (that has already broken down). The coordinates are supergalactic. sg_zz = 2.5 Mpc.

To be able to count the simulated isolated dwarf galaxies, we present in Figure 6 simulations with $k_{\mathrm{fs}} = 5.5$ Mpc^{-1}, at several supergalactic coordinates sg_zz. To count galaxies, we focus our attention on the blue contours with $\delta = 1.686$, and do not count very large perturbations with an irregular blue contour that would correspond to a large galaxy with satellites. Similar simulations are carried out for $k_{\mathrm{fs}} = 4.0$, 5.0, 5.5, 6.0, 6.5 and 20 Mpc^{-1}. The corresponding number densities of simulated isolated dwarf galaxies are presented in Table 1. The measured k_{fs} scales with the number of counted Local Field or simulated galaxies to the 1/3 power, and we add corresponding systematic uncertainties in the end. From Table 1, we obtain an upper bound to k_{fs}:

$$k_{\mathrm{fs}} \lesssim 5.6 \text{ Mpc}^{-1}. \tag{10}$$

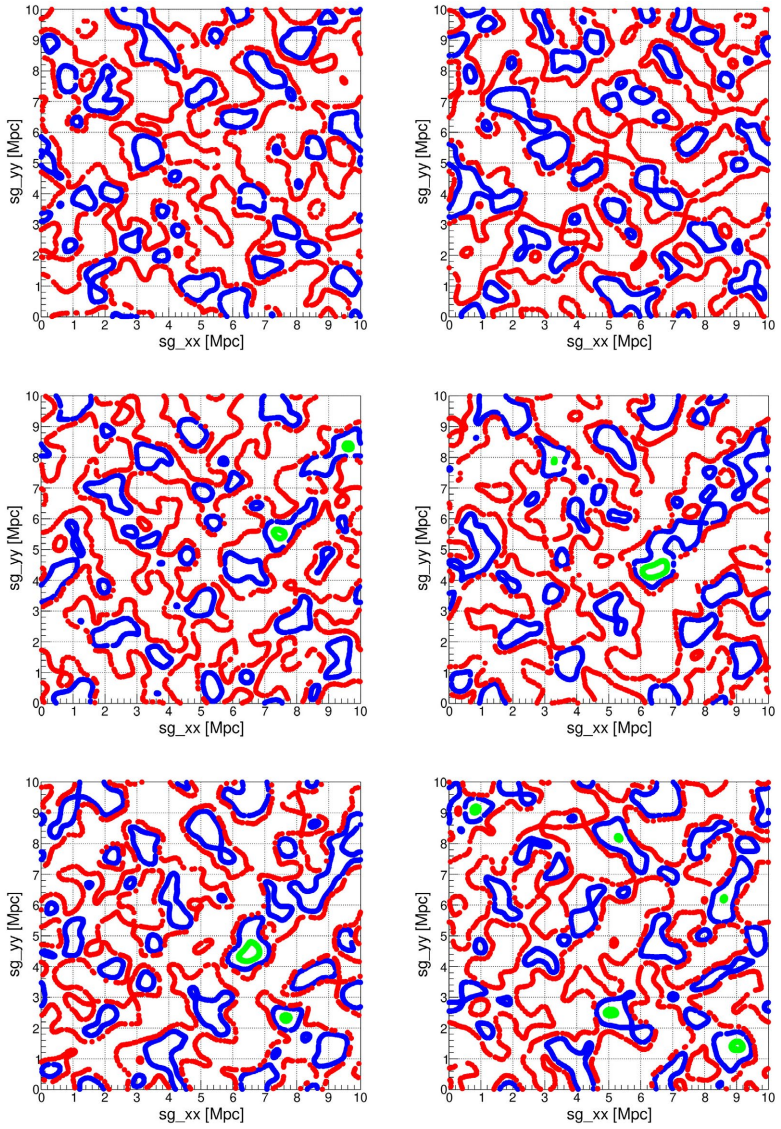

Figure 6. Simulations with $k_{\mathrm{fs}} = 5.5$ Mpc^{-1} and sg_zz = 2.0, 2.3, 2.6, 2.9, 3.1, and 3.4 Mpc. Shown are contours of constant relative over-density: $\delta(\boldsymbol{x}) = 0$ red, 1.69 blue, and 5 green, at redshift $z = 0$, in the linear approximation (that has already broken down).

Table 1. Comoving number densities of isolated dwarf galaxies obtained from linear simulations with several k_{fs}, to be compared with 0.743 ± 0.115 Mpc^{-3} isolated dwarf galaxies in the Local Field. This is before non-linear re-generation of the power spectrum at high wavevector k.

k_{fs} [Mpc^{-1}]	Number density [Mpc^{-3}]
4.0	0.41
5.0	0.49
5.5	0.70
6.0	0.96
6.5	1.51
20	25.00

6. Non-Linear Re-Generation of Small-Scale Perturbations

Non-linear re-generation of small-scale structure is a major effect that needs to be included in the analysis [11]-[14].

According to **Table 1** for $k_{fs} = 20$ Mpc^{-1}, the number density of isolated dwarf galaxies in the ΛCDM cosmology is approximately 25/0.743 = 34 times the observed number density in the Local Field! To reduce the cold dark matter predicted number density, we assume dark matter is warm. The reduction in number counts, obtained from the halo model and simulations, taking account of non-linear evolution, has the form [14].

$$\frac{n_{WDM}(M)}{n_{CDM}(M)} = \frac{1}{(1+M_{hm}/M)^{1.16}}. \tag{11}$$

The "half-mode" mass is $M_{hm} \equiv \frac{4}{3}\pi\bar{\rho}(\lambda_{hm}/2)^3$ with the half-mode length scale λ_{hm} defined such that $\tau(2\pi/\lambda_{hm}) \equiv 1/2$. From $\tau^2(k) = \exp(-k^2/k_{fs}^2)$, we obtain $k_{fs} = 2\pi/(\sqrt{\ln(4)}\lambda_{hm})$. M is the "halo mass", often defined as the mass enclosed in a region where $\langle\rho\rangle = 200\rho_{crit}$. **Table 2** presents the relation between m_{th}, M_{hm}, λ_{hm} and k_{fs}.

Table 2. The standard thermal relic warm dark matter mass m_{th} and the corresponding half-mode mass M_{hm}, from Table 1 of [14]. Also presented are the corresponding half-mode length scale λ_{hm} and the cut-off wavevector k_{fs} before the formation of the first galaxies.

m_{th} [keV]	M_{hm} [M$_\odot$]	λ_{hm} [Mpc]	k_{fs} [Mpc^{-1}]
∞	0	0	∞
1.25	4.2×10^9	0.6	9.1
1.0	8.8×10^9	0.7	7.1
0.75	2.3×10^{10}	1.0	5.2
0.5	8.8×10^{10}	1.6	3.3
0.25	8.8×10^{11}	3.5	1.5

Let us consider a dwarf galaxy with stellar mass $M_* \approx 2\times10^6\ \mathrm{M}_\odot$, see **Figure 2**. The corresponding halo mass, according to an extrapolation of Figure 11 of [15], is $M \approx 10^{10}\ \mathrm{M}_\odot$. Then, from (11), the needed warm dark matter suppression factor 0.743/25 is obtained with $M_{\mathrm{hm}} = 2\times10^{11}\ \mathrm{M}_\odot$, $\lambda_{\mathrm{hm}} = 2.1$ Mpc, and

$$k_{\mathrm{fs}} = 2.5\ \mathrm{Mpc}^{-1}, \tag{12}$$

before the formation of the first galaxies. This is our final estimate. Half of the non-linear re-generation correction from (10) to (12) will be assigned to one of the systematic uncertainties, see Section 9. This estimated uncertainty includes the uncertainty of Equation (11) when applied to the Local Field, and the uncertainty on M (up to a factor 6). This non-linear re-generation correction is the dominating uncertainty of the present analysis.

We need to cross-check that the dark matter is sufficiently cold so that a halo of mass $M \approx 10^{10}\ \mathrm{M}_\odot$ collapses. From Table 1 of [16], the needed $v_{hrms}(1)$ is $\lesssim$830 m/s, corresponding to the lower bound

$$k_{\mathrm{fs}} \gtrsim 0.6\ \mathrm{Mpc}^{-1}. \tag{13}$$

We note that $k_{\mathrm{fs}} \approx 2.5$ Mpc^{-1} satisfies this criterion.

7. Dwarf Galaxies Are Anomalous

Figure 7 presents the superposition of two graphs. One graph shows stellar mass distributions in units $10^{1.5} M_*$, and the other graph presents predicted distributions, for several values of k_{fs}, as a function of the linear Press-Schechter mass M_{PS}. The predictions are the Press-Schechter prediction and two ellipsoidal collapse extensions [17]-[20]. The superposition is useful if $10^{1.5} M_* \approx M_{\mathrm{PS}}$ as we have assumed in the past. With this approximation, predictions are in surprisingly good agreement with observations of stellar mass distributions and of ultra-violet luminosity distributions in a wide range of redshifts [20]. However, the approximation $10^{1.5} M_* \approx M_{\mathrm{PS}}$ breaks down at the high and low mass ends as shown in [15]. Dwarf galaxies do not follow the general distributions of larger galaxies. (This is also confirmed in [21]). In particular, to compare the predictions in **Figure 7** with dwarf galaxies, the red X's would have to be shifted to the right by about 2 orders of magnitude, as discussed in Section 6, see [15]. We might then arrive at the conclusion that dark matter is cold in agreement with the published limits on k_{fs} summarized in Figure 3 of [6]. However, we also need to understand the stellar mass distributions of large galaxies, and furthermore, cold dark matter obtains a great excess of dwarf galaxies as shown in **Table 1**.

The excess of dwarf galaxies relative to large galaxies in **Figure 7** may perhaps be understood by counting galaxies in **Figure 6** (a jump between first-generation galaxies and galaxies formed by bottom-up hierarchical evolution?), or may be due to an over-density of the Local Volume that reduces its expansion relative to the rest of the universe. We consider this possibility next.

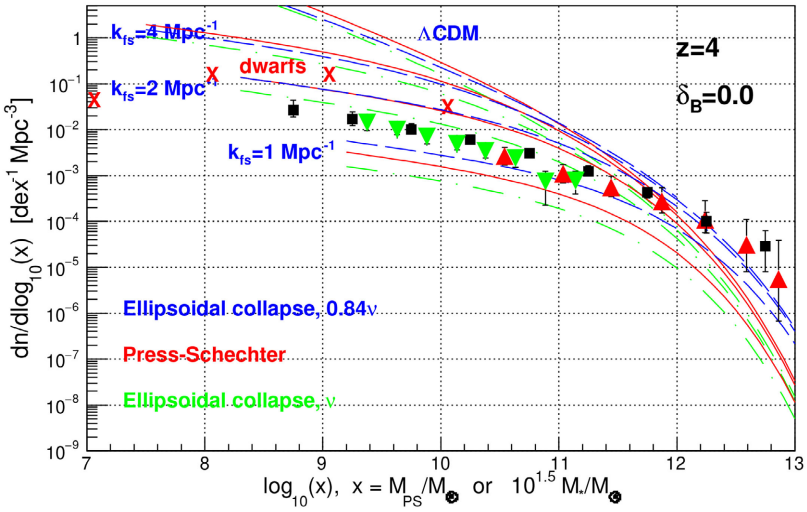

Figure 7. Superposition of two graphs at redshift $z = 4$. One graph presents stellar mass distributions in units $10^{1.5} M_*$ of isolated dwarf galaxies in the Local Field from the LSDB catalog [9] (red X's) (assuming the Local Field dwarfs are already in place at $z = 4$), and distributions obtained with the Hubble Space Telescope [22] (black squares), the continuity equation [23] (red triangles), and the James Webb Space Telescope (green triangles) [24]. The second graph presents the Press-Schechter [17] prediction and two ellipsoidal collapse extensions [18] [19] assuming a critical universe, for several values of k_{fs}, as a function of the linear Press-Schechter mass M_{PS}. See [20] for full details.

8. The Density of the Local Volume

The mean total (dark matter plus baryon) density in the Local Volume $\langle \rho_{m,\text{LV}} \rangle$ within 11 Mpc of the Milky Way is dominated by 21 large galaxies [25]. This mean is $\langle \rho_{m,\text{LV}} \rangle \approx 0.2 \rho_{\text{crit}}$, compared to the universe average $\langle \rho_m \rangle \approx 0.315 \rho_{\text{crit}}$. So, these measurements suggest the Local Field is underdense. The measured k_{fs} assuming $\langle \rho_{m,\text{LV}} \rangle = \langle \rho_m \rangle$ becomes multiplied by $\left(\langle \rho_m \rangle / \langle \rho_{m,\text{LV}} \rangle \right)^{1/3}$ due to the different expansion of the Local Volume with respect to the average universe.

However, an alternative estimate of $\langle \rho_{m,\text{LV}} \rangle$ can be obtained by comparing the stellar mass distribution of the isolated dwarf galaxies in the Local Field with that of galaxies at large, see **Figure 7**. This comparison suggests that the Local Field may have a matter over-density of a factor ≈ 5.

To be conservative, we will take $\langle \rho_{m,\text{LV}} \rangle$ to be in the range $0.15 \rho_{\text{crit}}$ to $1.6 \rho_{\text{crit}}$, corresponding to a k_{fs} correction factor between 1.3 and 0.58. This is the second dominating uncertainty of the present estimate of k_{fs}, see **Table 3**.

9. Results and Conclusions

We have estimated the cut-off wavevector k_{fs} due to warm dark matter free-streaming. It is defined as follows: $P_{\Lambda\text{CDM}}(k) \exp\left(-k^2/k_{\text{fs}}^2\right)$ is the linear density power spectrum, before first galaxies, *i.e.*, before re-generation of small-scale perturbations, referred to the present time. We have chosen the arguably simplest setting, namely the number density of isolated dwarf galaxies in the Local Field, that avoids a detailed, quantitative understanding of galaxy formation and evolution,

including satellites, in the warm dark matter scenario. The simple order-of-magnitude estimate (3) obtains $k_{\mathrm{fs}} \approx 5.7$ Mpc^{-1}. From the upper bound (10) and lower bound (13), we obtain

$$5.6\ \mathrm{Mpc}^{-1} \gtrsim k_{\mathrm{fs}} \gtrsim 0.6\ \mathrm{Mpc}^{-1}, \tag{14}$$

with an estimated confidence of 90%. Including the non-linear re-generation of small-scale structure obtains (12):

$$k_{\mathrm{fs}} = 2.5^{+1.8}_{-2.0}\ \mathrm{Mpc}^{-1}, \tag{15}$$

with 68% confidence. The breakdown of uncertainties is presented in **Table 3**. Combining these two results, we finally obtain

$$k_{\mathrm{fs}} = 2.5^{+1.8}_{-1.9}\ \mathrm{Mpc}^{-1}, \tag{16}$$

with 68% confidence. The corresponding comoving warm dark matter root-mean-square thermal velocity from (2) is

$$v_{h\mathrm{rms}}(1) = 278^{+880}_{-116}\ \mathrm{m/s}, \tag{17}$$

with 68% confidence. The measurement of $v_{h\mathrm{rms}}(1)$ allows the extrapolation of dark matter cosmology to the past [5] [26]. The corresponding "standard thermal relic mass" is $m_{\mathrm{th}} = 0.36^{+0.23}_{-0.26}$ keV. This result is in agreement with independent measurements summarized in [5], and in disagreement with published limits summarized in Table 3 of [6], and in Table 2 of [7], for example, $m_{\mathrm{th}} \gtrsim 10$ keV. Therefore, all limits and measurements, including the present one, need to be revised.

The bottom line is this: The ΛCDM prediction, e.g., the last panel in **Figure 4**, looks very different from the data in **Figure 1**.

The tightest limit on k_{fs} comes from the number of observed satellites of the Milky Way [6]. Such limits are obtained with simulations. These *same* simulations should also obtain the number density of dwarf galaxies in the Local Field. This cross-check would settle the discrepancy.

Table 3. Uncertainties of $k_{\mathrm{fs}} = 2.5^{+1.8}_{-2.0}$ Mpc^{-1} at 68% confidence.

Number of isolated dwarf galaxies in the Local Field	±0.17
Counts of isolated dwarf galaxies in the simulations	±0.2
Non-linear re-generation of small-scale structure	±1.6
Density of Local Volume (uncertainty of δ_{B})	$^{+0.70}_{-1.05}$
Long-wavelength cut-off of simulations	±0.5
Sum in quadrature	$^{+1.8}_{-2.0}$

Acknowledgements

All data in this article was obtained from the *Local Volume Database* (LVDB) catalog presented by Andrew B. Pace [9]. This catalog contains citations to each property of each dwarf galaxy, so a large community of astronomers have made the present investigation possible. Katya Gozman developed the handy application

(https://lvd-interactive.streamlit.app/) to visualize the galaxy distributions. I thank Karsten Müller for his early interest in this work and for many useful discussions.

Conflicts of Interest

The author declares no conflicts of interest regarding the publication of this paper.

References

[1] Navas, S., *et al.* (2024) The Review of Particle Physics. *Physical Review D*, **110**, Article ID: 030001.

[2] Hoeneisen, B. (2025) The Warm Dark Matter Plus Baryon Linear Power Spectrum. *International Journal of Astronomy and Astrophysics*, **15**, 264-281. https://doi.org/10.4236/ijaa.2025.153017

[3] Boyanovsky, D., de Vega, H.J. and Sanchez, N.G. (2008) Dark Matter Transfer Function: Free Streaming, Particle Statistics, and Memory of Gravitational Clustering. *Physical Review D*, **78**, Article ID: 063546. https://doi.org/10.1103/physrevd.78.063546

[4] Viel, M., Lesgourgues, J., Haehnelt, M.G., Matarrese, S. and Riotto, A. (2005) Constraining Warm Dark Matter Candidates Including Sterile Neutrinos and Light Gravitinos with WMAP and the Lyman-α Forest. *Physical Review D*, **71**, Article ID: 063534. https://doi.org/10.1103/physrevd.71.063534

[5] Hoeneisen, B. (2024) Measurements of the Dark Matter Mass, Temperature and Spin. *International Journal of Astronomy and Astrophysics*, **14**, 184-202. https://doi.org/10.4236/ijaa.2024.143012

[6] Liu, B., Shan, H. and Zhang, J. (2024) New Galaxy UV Luminosity Constraints on Warm Dark Matter from JWST. *The Astrophysical Journal*, **968**, Article 79. https://doi.org/10.3847/1538-4357/ad4ed8

[7] Hoeneisen, B. (2025) Warm Dark Matter Studies with Spiral Galaxy Data. *International Journal of Astronomy and Astrophysics*, **15**, 336-355. https://doi.org/10.4236/ijaa.2025.154021

[8] Xu, K., *et al.* (2025) PAC in DESI. I. Galaxy Stellar Mass Function into the $10^6 M_\odot$ Frontier. arXiv: 2503.01948.

[9] Pace, A.B. (2024) The Local Volume Database: A Library of the Observed Properties of Nearby Dwarf Galaxies and Star Clusters. arXiv: 2411.07424.

[10] Weinberg, S. (2008) Cosmology. Oxford University Press.

[11] Parimbelli, G., Scelfo, G., Giri, S.K., Schneider, A., Archidiacono, M., Camera, S., *et al.* (2022) Mixed Dark Matter: Matter Power Spectrum and Halo Mass Function. arXiv: 2106.04588.

[12] MacInnis, A. and Sehgal, N. (2024) CMB-HD as a Probe of Dark Matter on Sub-Galactic Scales. arXiv: 2405.12220.

[13] Despali, G., Moscardini, L., Nelson, D., Pillepich, A., Springel, V. and Vogelsberger, M. (2025) Introducing the AIDA-TNG Project: Galaxy Formation in Alternative Dark Matter Models. *Astronomy & Astrophysics*, **697**, A213. https://doi.org/10.1051/0004-6361/202553836

[14] Schneider, A., Smith, R.E., Macciò, A.V. and Moore, B. (2012) Nonlinear Evolution of Cosmological Structures in Warm Dark Matter models. arXiv: 1112.0330.

[15] Behroozi, P.S., Conroy, C. and Wechsler, R.H. (2010) A Comprehensive Analysis of Uncertainties Affecting the Stellar Mass-Halo Mass Relation for $0 < z < 4$. *The Astro-*

physical Journal, **717**, 379-403. https://doi.org/10.1088/0004-637x/717/1/379

[16] Hoeneisen, B. (2022) Measurement of the Dark Matter Velocity Dispersion with Galaxy Stellar Masses, UV Luminosities, and Reionization. *International Journal of Astronomy and Astrophysics*, **12**, 258-272. https://doi.org/10.4236/ijaa.2022.123015

[17] Press, W.H. and Schechter, P. (1974) Formation of Galaxies and Clusters of Galaxies by Self-Similar Gravitational Condensation. *The Astrophysical Journal*, **187**, 425-438. https://doi.org/10.1086/152650

[18] Sheth, R.K. and Tormen, G. (1999) Large-Scale Bias and the Peak Background Split. *Monthly Notices of the Royal Astronomical Society*, **308**, 119-126. https://doi.org/10.1046/j.1365-8711.1999.02692.x

[19] Sheth, R.K., Mo, H.J. and Tormen, G. (2001) Ellipsoidal Collapse and an Improved Model for the Number and Spatial Distribution of Dark Matter Haloes. *Monthly Notices of the Royal Astronomical Society*, **323**, 1-12. https://doi.org/10.1046/j.1365-8711.2001.04006.x

[20] Hoeneisen, B. (2024) Are James Webb Space Telescope Observations Consistent with Warm Dark Matter? *International Journal of Astronomy and Astrophysics*, **14**, 45-60. https://doi.org/10.4236/ijaa.2024.141003

[21] Moore, S.G., Cole, S., Wilson, M., Norberg, P., *et al.* (2025) DESI DR2 Galaxy Luminosity Functions. arXiv: 2511.01803.

[22] Song, M., Finkelstein, S.L., Ashby, M.L.N., Grazian, A., Lu, Y., Papovich, C., *et al.* (2016) The Evolution of the Galaxy Stellar Mass Function at $z = 4$ - 8: A Steepening Low-Mass-End Slope with Increasing Redshift. *The Astrophysical Journal*, **825**, Article 5. https://doi.org/10.3847/0004-637x/825/1/5

[23] Lapi, A., Mancuso, C., Bressan, A. and Danese, L. (2017) Stellar Mass Function of Active and Quiescent Galaxies via the Continuity Equation. *The Astrophysical Journal*, **847**, 13. https://doi.org/10.3847/1538-4357/aa88c9

[24] Navarro-Carrera, R., Rinaldi, P., Caputi, K.I., Iani, E., Kokorev, V. and van Mierlo, S.E. (2023) Constraints on the Faint End of the Galaxy Stellar Mass Function at $z \simeq 4$ - 8 from Deep JWST Data. arXiv: 2305.16141.

[25] Karachentsev, I.D. and Telikova, K.N. (2018) Stellar and Dark Matter Density in the Local Universe. arXiv: 1810.06326.

[26] Hoeneisen, B. (2019) A Study of Dark Matter with Spiral Galaxy Rotation Curves. *International Journal of Astronomy and Astrophysics*, **9**, 71-96. https://doi.org/10.4236/ijaa.2019.92007